Extracellular matrix glycoproteins and diffusion barriers in human astrocytic tumours

J. Zámečník*, L. Vargová†‡, A. Homola†‡, R. Kodet* and E. Syková†‡§

Department of Pathology and Molecular Medicine, †Department of Neuroscience, ‡Center for Cell Therapy and Tissue Repair, Charles University, 2nd Medical Faculty, Prague, Czech Republic, §Institute of Experimental Medicine, Academy of Sciences of the Czech Republic, Prague, Czech Republic

J. Zámečník, L. Vargová, A. Homola, R. Kodet and E. Syková (2003) *Neuropathology and Applied Neurobiology*, **30**, 338–350

Extracellular matrix glycoproteins and diffusion barriers in human astrocytic tumours

The extracellular matrix (ECM) and changes in the size and geometry of the extracellular space (ECS) in tumour tissue are thought to be of critical importance in influencing the migratory abilities of tumour cells as well as the delivery of therapeutic agents into the tumour. In 21 astrocytic neoplasms, the ECM composition was investigated *in situ* by the immunohistochemical detection of ECM glycoproteins (tenascin, laminin, vitronectin, fibronectin, collagen types I–VI). To explain the changes in ECS size and to detect barriers to diffusion in the tumour tissue, the ECM composition, the cellularity, the density of glial fibrillary acidic protein (GFAP)-positive tumour cell processes and the proliferative activity of the tumours were compared with the size and geometry of the ECS. The ECS volume fraction and the complex of hindrances to diffusion in the ECS (i.e. the tortuosity) were revealed by the real-time iontophoretic tetramethylammonium method. Increased proliferative activity of the tumours correlated with increased ECS volume fraction and tortuosity. The tortuosity of the tumour tissue was not significantly influenced by tumour cell density. Higher tortuosity was found in low-grade astrocytomas associated with the presence of a dense net of GFAP-positive fibrillary processes of the tumour cells. The increase in tortuosity in high-grade tumours correlated with an increased accumulation of ECM molecules, particularly of tenascin. We conclude that the increased malignancy of astrocytic tumours correlates with increases in both ECS volume and ECM deposition.

Keywords: glioma, diffusion, extracellular matrix, tenascin, vitronectin, collagen

Introduction

The process of tumour progression, which comprises changes in the expression of extracellular matrix (ECM) components, cell adhesion molecules and proteolytic enzymes [1,2], also inevitably leads to changes in extracellular space (ECS) size and geometry. The ECS of the brain is an important microenvironment of the nervous system and a communication channel for nerve cells [3], and it dynamically changes during neuronal activity, development, ageing and some pathological states [4]. Although changes in the ECS are thought to be of critical importance for influencing not only the migratory abilities of tumour cells but also the delivery of neuroactive substances or therapeutic drugs into the tumour, there is only limited information available concerning the ECS in neoplasms of the brain.

The structure (size and geometry) of the ECS in nervous tissue can be accurately determined by the tetramethylammonium (TMA⁺) real-time iontophoretic method,

Correspondence: Eva Syková, Department of Neuroscience, Institute of Experimental Medicine AS CR, Vídeňská 1083, 142 20 Prague 4, Czech Republic. Tel: +420 241 062204; Fax: +420 241 062783/+420 224 436799; E-mail: sykova@biomed.cas.cz

which uses TMA$^+$ as an extracellular marker and follows its diffusion in the ECS by TMA$^+$-selective microelectrodes [5]. Diffusion in the ECS of the nervous system is constrained mainly by two factors [6]: the restricted volume of the selected tissue available for diffusing particles, that is, the ECS volume fraction α (α = ECS volume/total tissue volume), and tortuosity λ (λ^2 = free/apparent diffusion coefficient), a factor describing the hindrances to diffusion in the ECS [7].

Our recent study on human primary brain tumours revealed critical changes in the diffusion parameters in brain tumours, namely an increase in both volume fraction and tortuosity [8]. The diffusion of molecules in the ECS may be hindered by membrane obstructions, fine cell processes and by macromolecules forming the ECM [9]. Previous studies indicate that changes in ECS volume and an increase in diffusion barriers can be evoked by astrogliosis [7,10] or by changes in ECM content [7,9]. It has been shown that the ECM composition of brain tumours is changed in comparison with normal brain tissue (for review see [2,11,12]). However, present knowledge about ECM composition in glial tumours is based mostly on studies of permanent cell lines or spheroids; considerably less work has been done on the *in situ* characterization of the presence and distribution of ECM molecules in biopsy specimens [2,11,12].

We therefore studied biopsy specimens of human astrocytic neoplasms, the most frequent primary brain tumours [13], in order to detect diffusion barriers and to explain the observed changes in ECS size and geometry. We investigated the relationships between the size and geometry of the ECS and the histological tumour structure, namely the cellularity, the density of glial fibrillary acidic protein (GFAP)-positive tumour cell processes, the proliferative activity of the tumour cells and the ECM composition. As antibodies against ECM glycoproteins suitable for paraffin-embedded material have recently become available, we investigated the expression of a spectrum of the larger ECM molecules, including tenascin, laminin, vitronectin, fibronectin and collagen types I–VI.

Materials and methods

Tissue samples for structural and immunohistochemical analysis and diffusion measurements were obtained during surgical resections of brain tumours in 21 previously untreated male (n = 12) and female (n = 9) patients, 2–75 years old (mean 33.8 years). Because of the previously

demonstrated diffusion anisotropy in white matter [3,5,14], cortical tissue from four patients aged 10–27 years that was resected during the surgical treatment of temporal lobe epilepsy as a result of hippocampal sclerosis and that did not reveal any structural changes was used as a control.

Slice preparation for the diffusion measurements

Prior to histological and immunohistochemical analysis, diffusion measurements were performed on freshly resected brain tissue samples. Immediately after tissue removal, samples were placed into ice-cold, bicarbonate-buffered transport solution bubbled with 95% O$_2$ and 5% CO$_2$ of the following composition: 134 mM NaCl, 1.25 mM K$_2$HPO$_4$, 26 mM NaHCO$_3$, 3.3 mM MgCl$_2$ and 20 mM glucose. Within 30 min after surgery, 400 μm thick slices were cut in ice-cold solution using a Vibratome. A slice was then placed into the experimental chamber and perfused with a continuously bubbled (95% O$_2$ and 5% CO$_2$) calcium-containing solution (134 mM NaCl, 1.25 mM K$_2$HPO$_4$, 26 mM NaHCO$_3$, 1.3 mM MgCl$_2$, 2 mM CaCl$_2$, 20 mM glucose) at a flow rate of 10 ml/min. In the experimental chamber, the slice was slowly warmed up, and measurements were performed at room temperature (22–24°C) at various locations in the slice at a depth of 200 μm.

Diffusion measurements

The ECS diffusion parameters ECS volume fraction (α), tortuosity (λ) and nonspecific cellular uptake (k'), a factor describing the loss of a substance across cell membranes, were determined by the real-time iontophoretic method developed by Nicholson and Phillips [6] and described in detail previously [15]. In brief, an extracellular marker that is restricted to the extracellular compartment is used, such as TMA$^+$ (molecular weight = 74.1), to which cell membranes are relatively impermeable. TMA$^+$ is administered into the tissue by iontophoresis and its concentration in the ECS, measured by a TMA$^+$-ion selective microelectrode (ISM), is inversely proportional to the ECS volume. Double-barreled TMA$^+$-ISMs were prepared by a procedure described in detail previously [16]. In brief, the tip of the ion-sensitive barrel was filled with an ion exchanger (Corning 477317), and the rest of the barrel was back-filled with 100 mM TMA chloride. The reference barrel contained 150 mM NaCl. To determine the slope and

interference, TMA$^+$-ISMs were calibrated in a sequence of solutions of 150 mM NaCl + 3 mM KCl with the addition of the following concentrations of TMA chloride (mM): 0.1, 0.3, 1.0, 3.0 and 10.0. The shank of the iontophoretic pipette was bent so that it could be aligned parallel to that of the ISM and was back-filled with 100 mM TMA chloride. An electrode array was made by gluing together a TMA$^+$-ISM and an iontophoretic micropipette with a tip separation of 100–200 μm (Figure 1). The iontophoresis parameters were +20 nA bias current (continuously applied to maintain a constant electrode transport number) with an +180 nA current step of 60 s duration to generate the diffusion curve. The three parameters were extracted by a nonlinear curve-fitting simplex algorithm operating on the diffusion curve assuming that TMA$^+$ spreads out with spherical symmetry [6].

Prior to tissue measurements, diffusion curves were recorded in 0.3% agar gel (Difco, Kansas City, MO, USA) dissolved in a solution of 150 mM NaCl, 3 mM KCl and 1 mM TMA chloride. In dilute agar α and λ are by definition set to 1 and k' is set to 0; the electrode transport number (n) and the free TMA$^+$ diffusion coefficient (D) are extracted by curve fitting. Knowing n and D, the parameters α, λ and k' can be obtained when the experiment is repeated in a tissue sample.

Measurements were performed in 2–6 slices from each tissue sample. In each slice, at least two diffusion measurements were conducted in 2–3 different locations and the obtained results were averaged. In this study, we performed 51 measurements in 10 slices obtained from five patients; the diffusion measurements from the remaining patients ($n = 16$) were published previously [8]. In the current study, we used the tissue samples from all patients ($n = 21$) for further morphological and immunohistochemical analysis.

Morphology and tumour grading

Tissue samples used for diffusion measurements as well as the remaining resected tissue were fixed in 10% buffered formalin and embedded in paraffin. To determine the morphological features of the tissue and for tumour typing, routine haematoxylin-eosin staining was performed. Astrogliosis or the astrocytic nature of the neoplasm was demonstrated by immunohistochemical staining with antibodies directed against GFAP as described in the following section. The tumours were classified and graded according to the criteria outlined by the World Health Organization (WHO) [13]. The histological structure of the slices in the locations where the ECS diffusion parameters were measured was evaluated and correlated with the diffusion measurements. The results of diffusion measurements made in areas from near the edge of the tumour, from the vicinity of large vessels or in areas with
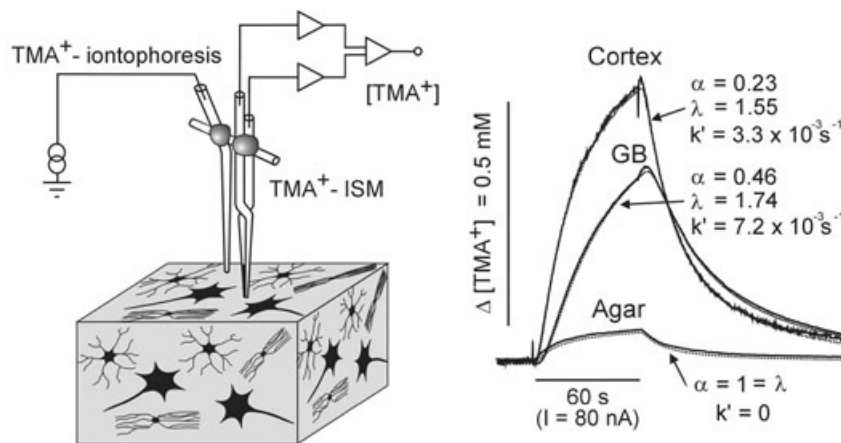
Figure 1. Experimental setup for the measurement of extracellular space (ECS) diffusion parameters (left) and representative Tetramethylammonium (TMA$^+$)-diffusion curves with the corresponding values of the parameters obtained in agar gel, control neocortical tissue and a glioblastoma (right). TMA$^+$ was iontophoresed into the tissue by an iontophoretic micropipette, and its concentration was measured by a TMA$^+$ ion-selective microelectrode (ISM). To stabilize the intertip distance of the electrode array, an iontophoretic micropipette and a TMA$^+$-selective microelectrode were glued together with dental cement. In the brain, where diffusion is constrained by various barriers and restricted to the ECS, the amplitude of the diffusion curve is much higher and its shape differs from the diffusion curve measured in agar gel, where by definition $\alpha = \lambda = 1$ and $k' = 0$. α, ECS volume fraction; λ, tortuosity; GB, glioblastoma.

haemorrhage were excluded. In glioblastomas, a consistent feature of which were areas of coagulative necroses, only measurements in viable cellular regions were used for statistical analysis (for details see [8]).

Immunohistochemistry

Serial tissue sections 4 µm thick were recut from the appropriate paraffin blocks for immunohistochemical purposes, approximately at the level where diffusion measurements were performed. Tissue sections were deparaffinized and rehydrated. Following cooling for 20 min and blocking of endogenous peroxidase activity, sections were incubated overnight at 4°C with antibodies directed against tumour cell proliferation markers, GFAP or ECM glycoproteins (tenascin, vitronectin, laminin, fibronectin and collagen types I–VI). To avoid background staining, the optimal dilutions of the primary antibodies and tissue section pretreatments were determined prior to the study by test stainings using checkerboard titrations on normal brain, kidney and skin tissues. We used the immunohistochemical detection of the Ki-67 antigen (MIB-1) [17] and phospho-topoisomerase II-α (topo-IIα) [18] as proliferation markers. The antigen–antibody complexes were visualized by biotin-streptavidin detection systems (LSAB2 System, HRP, Dako, Glostrup, Denmark; cat. no. K0675; ChemMate Detection kit, HRP, Dako, cat. no. K5001). Chromogenic development was performed using 3,3′-diaminobenzidine (Fluka Chemie GmbH, Steinheim, Germany). Further details concerning the antibodies, dilutions and pretreatment methods used are indicated in Table 1. Positive and negative controls were used in each assay.

Evaluation of histopathological and immunohistochemical features

Each slice in which diffusion measurements were performed was studied under high-power magnification (high-power field, HPF; ×400, area comprising 0.017 mm^2). The cell density was counted exactly in at least 10 HPFs of serial sections in viable regions of the tumours and was expressed as the mean value for one HPF. Mitotic activity was expressed as the mean mitotic count value for 10 HPFs. Vascular proliferation was defined as an increase in the number of vessels in a section and/or as a hyperplasia of the endothelial cells forming multilayered small vessels. The presence of such hyperplastic vasculature was graded as excessive (+++), moderate (++), mild (+) or absent (–).

The results of immunostaining with antibodies directed against MIB-1 and topo-IIα antigens were evaluated in the areas with the most intensive staining and were expressed as labelling indices (LIs), defined as the percentages of immunoreactive nuclei divided by the total number of tumour cells in the evaluated area. For each evaluation, at least 1000 cells in at least five HPFs were counted.

Table 1. Antibodies and detection kits used for the immunohistochemical studies

Antigen (antibody)	Source	Dilution	Pretreatment, detection kit
Glial fibrillary acidic protein (MM, clone 6F2)	Dako	1 : 1000	Microwave pretreatment*
Tenascin (MM, clone BC-24)	Sigma Aldrich	1 : 500	Microwave pretreatment*
Laminin (MM, clone LAM-89)	Sigma Aldrich	1 : 500	40 min enzyme predigestion*
Vitronectin (MM, clone BV2)	Chemicon	1 : 100	Microwave pretreatment†
Fibronectin (MM, clone IST-4)	Sigma Aldrich	1 : 50	30 min enzyme predigestion, microwave pretreatment†
Type I collagen (RP, cat. no. 2150-0020)	Biotrend, GmbH	1 : 10	40 min enzyme predigestion*
Type II collagen (MM, cat. no. NCL-COLL-IIp)	Novocastra	1 : 20	30 min enzyme predigestion*
Type III collagen (MM, cat. no. AM167-5M)	Biogenex	1 : 100	30 min enzyme predigestion*
Type IV collagen (MM, clone CIV 22)	Dako	1 : 50	Microwave pretreatment*
Type V collagen (MM, clone V-3C9)	Chemicon	1 : 150	Microwave pretreatment*
Type VI collagen (MM, clone VI-26)	Chemicon	1 : 150	Microwave pretreatment*
Ki-67 (MM, clone MIB-1)	Dako	1 : 100	Microwave pretreatment*
Phospho-topoisomerase II-α (MM, clone PT/3D4)	Immunotech	1 : 100	– *

MM, mouse monoclonal antibody; RP, rat polyclonal antibody.
*LSAB2 System HRP detection kit.
†ChemMate detection kit.

The intensity of the immunohistochemical staining using antibodies directed against ECM glycoproteins was evaluated in the studied areas in two separate regions, in association with the blood vessels and also in the ECS surrounding the tumour cells, independently by two observers, and consensus was reached for the scoring of the definitive staining intensity. To exclude the evaluation of equivocal staining, the evaluations were performed in two steps: first in sections without counterstaining, then the precise localization and distribution of the evaluated glycoprotein were confirmed after counterstaining with Harris' haematoxylin. The presence of ECM glycoproteins in the pericellular spaces was classified as strong (++) or weak (+) fibrillar or dot immunopositivity or as negative (−). The diffuse or focal pattern of the distribution was also noted. The percentage of immunopositive small blood vessel walls or capillaries was determined for each studied ECM glycoprotein and expressed semiquantitatively: no positivity in blood vessels (−), positive in less than one-half of blood vessels (+), positive in more than one-half of blood vessels (++), or positive in all blood vessels (+++). The distribution of the immunoreactions in the blood vessel walls was also noted. The density of GFAP immunostaining in astrocytic tumours was semiquantitatively graded as a loose (+), moderately dense (++) or very dense (+++) net of GFAP-positive tumour cell processes. In the sections of control cortex, only scarce GFAP-positive glial processes were observed, and the results were classified as negative (−).

Statistical analysis

Associations between numeric variables were assessed via Spearman's rank correlation analysis (with correlation coefficient estimate, r), and associations between categorical and numeric variables were assessed via the Mann–Whitney test. All analytical work was performed using the analytical software SPSS (version 10, SPSS Inc., Chicago, IL, USA). Probability (P) values < 0.05 were considered significant.

Results

Human temporal cortex

In control healthy temporal lobe neocortex (cases 1–4), immunohistochemical staining revealed rare GFAP-positive astrocytes, mostly in the subpial and perivascular regions. The walls of capillaries and blood vessels were free of tenascin; however, clearly distinguishable fine fibrils of tenascin were detected in all the studied cases in the outer regions of layer I of the cortex and glial limitans externa. Weak diffuse fibrillary tenascin immunopositivity was also noted in the ECS of the subcortical white matter (Figure 2). In the deep cortical tissue, where the diffusion measurements were performed, no tenascin accumulation was observed. The basement membranes of all of the few small blood vessels and capillaries found were positive for type IV collagen, laminin and fibronectin. Collagens types II, V and VI were pronounced in the adventitia of larger blood vessel, while fibres of collagen types I and III were present in their fibromuscular coat. Immunopositivity for collagen types I–III, V and VI was also observed in the connective tissues of leptomeninges. However, no deposits of either vitronectin or collagen types I–III, V or VI were detected in the deeper cortical areas that were the sites of the diffusion measurements.

ECS diffusion parameter measurements were performed in layers II–IV of the lateral cortex of the temporal lobe (see Table 2). The average values of α and λ in control tissue were 0.24 and 1.55, respectively.

Pilocytic astrocytomas (WHO grade I)

The pilocytic astrocytomas (cases 5–9) were all typical neoplasms with a varying proportion of compacted regions of bipolar cells with Rosenthal fibres and loose textured multipolar cells with microcysts and eosinophilic granular bodies. Cell density, mitotic activity and the MIB-1 and topo-IIα LIs were very low. All tumour cells were GFAP-positive; however, the density of GFAP-positive fibrillary processes of the tumour cells was lower in loose textured areas with microcysts and moderate to strong in compacted regions. No extracellular deposits of ECM glycoproteins were detected (Figure 3). The basement membranes of all tumour blood vessels were intensely positive for type IV collagen, laminin and fibronectin. In comparison with the control temporal cortex, ECS volume fraction in pilocytic astrocytomas was significantly higher [Mann–Whitney test (MW); $P < 0.001$] while the tortuosity values did not significantly differ from the control values (see Table 2).

Table 2. Histology results, the extracellular matrix (ECM) glycoproteins present in the extracellular space (ECS) surrounding tumour cells and the ECS diffusion parameters, the presence of hyperplastic vasculature and the expression of ECM molecules associated with vascular elements

No.	Age, sex	Proliferation	TCD	GFAP	ECM-ECS TN	ECM-ECS VT	Diffusion parameters α	Diffusion parameters λ	Diffusion parameters $k'(\times 10^3\,s^{-1})$	HV	ECM associated with vascular elements TN	FB	LM	C-IV	C-II	C-V	C-VI
Control tissues																	
1*	17, F	0	–	–	–	–	0.24±0.01	1.48±0.02	8.57±0.32	–	–	–	+++	+++	–	–	–
2*	17, F	0	–	–	–	–	0.24±0.01	1.50±0.02	1.87±0.16	–	–	+++	+++	+++	–	–	–
3*	10, F	0	–	–	–	–	0.24±0.01	1.61±0.01	2.57±0.47	–	–	+++	+++	+++	–	–	–
4*	10, F	0	–	–	–	–	0.23±0.01	1.65±0.01	1.41±0.05	–	–	+++	+++	+++	–	–	–
Pilocytic astrocytomas (grade I)																	
5*	4, F	0.4–1.3–0	118.5	++	–	–	0.37±0.01	1.52±0.03	2.59±0.78	–	–	+++	+++	+++	–	–	–
6*	2.5, F	0.6–0.2–0	123.2	+++	–	–	0.35±0.01	1.61±0.01	3.31±0.23	–	–	+++	+++	+++	–	–	–
7*	17, M	1.6–2.2–0	79.0	+	–	–	0.38±0.01	1.37±0.01	7.80±0.72	–	–	+++	+++	+++	–	–	–
8*	7, M	1.6–2.1–0	99.9	++	–	–	0.38±0.01	1.52±0.05	6.90±0.82	–	–	+++	+++	+++	–	–	–
9*	10, M	2.6–3.2–1	112.6	++	–	–	0.41±0.02	1.49±0.01	4.96±0.26	–	–	+++	+++	+++	–	–	–
Astrocytomas (grade II)																	
10	24, F	2.1–1.7–1	98.1	++	–	–	0.30±0.01	1.45±0.01	7.82±0.72	–	–	+++	+++	+++	–	–	–
11*	26, M	7.2–7.6–3	100.2	+++	–	–	0.29±0.01	1.57±0.02	3.13±0.62	–	–	+++	+++	+++	–	–	–
12*	9, M	6.6–7.2–1	112.7	+++	–	–	0.31±0.02	1.69±0.02	3.70±0.50	–	–	+++	+++	+++	–	–	–
13*	12, M	3.8–4.4–0	84.6	+++	–	–	0.27±0.01	2.12±0.07	7.13±1.03	–	–	+++	+++	+++	–	–	–
14	28, M	3.9–3.2–3	87.7	++	–	–	0.28±0.01	1.52±0.01	7.00±0.27	–	–	+++	+++	+++	–	–	–
Anaplastic astrocytomas (grade III)																	
15*	47, F	19.4–16.2–11	223.2	++	F+	–	0.41±0.01	1.67±0.03	5.12±0.43	–	+	++	+++	+++	–	–	–
16*	8, F	31.2–32.0–24	268.6	++	F+	–	0.52±0.02	1.67±0.03	5.49±0.78	–	++	+	+++	+++	–	–	–
17*	24, F	33.4–35.4–26	196.2	++	D++	F+	0.53±0.01	1.87±0.13	9.93±1.13	–	++	+	+++	+++	–	–	–
Glioblastomas (grade IV)																	
18	66, M	12.3–14.5–12	296.7	+	–	–	0.46±0.01	1.44±0.01	9.28±1.15	+	–	++	+++	+++	+	+	+
19*	68, F	22.8–18.6–15	329.1	+	D+	F+	0.40±0.01	1.72±0.03	9.93±0.76	++	+++	+	+++	+++	+	+	+
20*	43, M	23.0–24.4–21	232.1	+	D++	F+	0.42±0.01	1.86±0.03	7.87±0.98	++	++	+	+++	+++	++	+	+
21*	54, M	24.4–21.4–14	280.2	+	D++	F+	0.40±0.01	1.85±0.03	4.40±0.52	+++	+++	–	+++	+++	++	+	+
22	75, M	27.3–29.5–28	311.4	+	D+	–	0.48±0.02	1.67±0.01	6.51±0.96	++	+++	+	+++	+++	++	++	++
23*	62, M	29.6–30.4–23	215.3	+	–	–	0.56±0.01	1.35±0.04	2.64±0.05	+	–	+	+++	+++	+	+	+
24	63, M	36.8–32.1–27	220.9	++	D++	–	0.46±0.01	1.74±0.01	7.27±0.45	+	+++	++	+++	+++	++	++	++
25*	62, F	52.2–45.4–32	298.3	+	D++	–	0.58±0.02	1.69±0.03	5.19±0.32	++	+++	–	+++	+++	++	+	+

*The diffusion measurements from the case were published previously [8].

F, female; M, male.

Proliferation: MIB-1 labelling index – topoisomerase II-α labelling index – mitotic count per 10 high-power fields.

TCD, tumour cell density.

GFAP, fibrillary net of GFAP-positive tumour cell processes: loose (+), moderately dense (++), or very dense (+++).

ECM-ECS: ECM glycoproteins present in the extracellular space surrounding tumour cells; TN, tenascin; VT, vitronectin; absent (–), weak (+) or strong (++) immunopositivity; F, focal; D, diffuse.

α, ECS volume fraction; λ, ECS tortuosity; k', nonspecific uptake.

HV, hyperplastic vasculature: excessive (+++), moderate (++), mild (+) or absent (–).

ECM associated with vascular elements: TN, tenascin; FB, fibronectin; LM, laminin; C-II, type II collagen; C-IV, type IV collagen; C-V, type V collagen; C-VI, type VI collagen; no positivity in blood vessels (–), positive in less than one-half of blood vessels (+), positive in more than one-half of blood vessels (++), and positive in all blood vessels (+++).
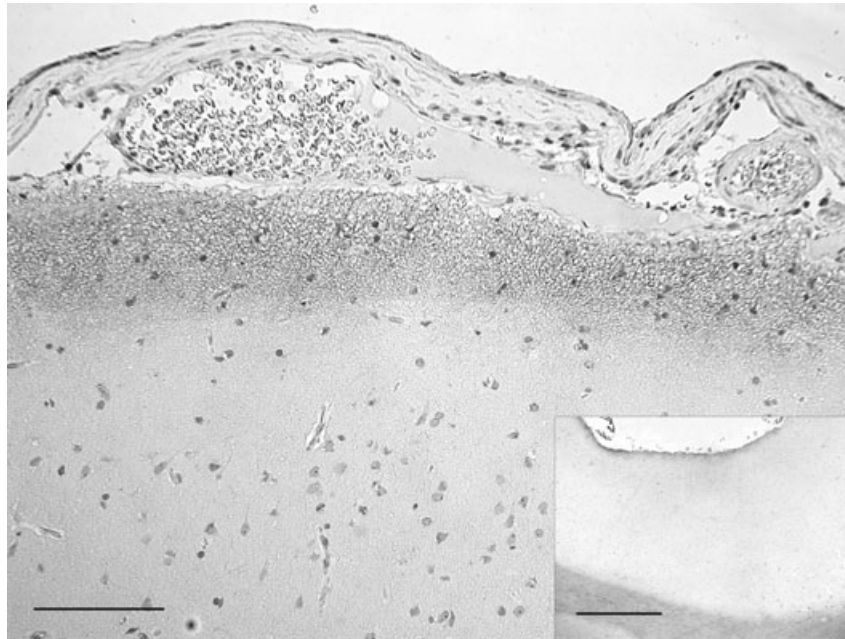
Figure 2. Tenascin immunopositivity in the outer region of layer I of the cortex and glial limitans externa (counterstained slightly with haematoxylin, scale bar = 100 µm). Inset: immunoperoxidase staining for tenascin in normal temporal cortex at low magnification (counterstained slightly with haematoxylin, scale bar = 1000 µm).

Astrocytomas (WHO grade II)

Astrocytomas (cases 10–14) exhibited a modest increase in cellularity. Anti-GFAP immunostaining revealed a dense fibrillary network of numerous fine, long-branched GFAP-positive processes of irregularly distributed neoplastic astrocytes (Figure 3). Proliferative activity was very low, and vascular proliferations were absent. The expression and distribution of the studied ECM glycoproteins were the same as observed in pilocytic astrocytomas (Figure 3). The average value of α was significantly higher than in control tissue (MW; $P < 0.001$) but lower than that in pilocytic astrocytomas (MW; $P < 0.001$). The generally increased tortuosity varied greatly among the cases (Table 2): extremely high tortuosity (2.12) was observed in case 13, the dominant histological feature of which was a dense network of fascicularly arranged GFAP-positive tumour cell processes.

Anaplastic astrocytomas and glioblastomas (WHO grade III and IV)

A notably increased cellularity, distinct nuclear and cellular pleomorphism and marked mitotic activity together with increased proliferative activity as demonstrated by MIB-1 and topo-IIα LIs were characteristics of high-grade astrocytic tumours. The viable regions of glioblastomas (cases 18–25) differed from anaplastic astrocytomas (cases 15–17) by the presence of various degrees of vascular proliferation, often forming glomeruloid formations.

Anti-GFAP immunostaining demonstrated that all tumour cells in both anaplastic astrocytomas and glioblastomas were GFAP-positive, but that they had distinctly shorter processes with reduced branching when compared with low-grade tumours (Figure 3). In nine of 11 high-grade astrocytomas, a varying degree of tenascin production was observed in both the dilated spaces surrounding the neoplastic astrocytes and in the walls of blood vessels, being mostly focal in anaplastic astrocytomas and diffuse in glioblastomas. In four cases of high-grade astrocytomas, focal deposits of vitronectin were detected in the ECS (Figure 3). A range of ECM glycoproteins was observed in the basement membranes of blood vessels in high-grade astrocytomas. A significant decrease in the intensity and percentage of fibronectin-positive blood vessel basal membranes was noted, and in two glioblastoma cases no fibronectin expression was found (Figure 4). An accumulation of tenascin in the blood vessel walls was observed in nine of 11 cases of high-grade tumours. Both type IV collagen and laminin were detected

$$\alpha = 0.24 \qquad \alpha = 0.37 \qquad \alpha = 0.31 \qquad \alpha = 0.42$$
$$\lambda = 1.50 \qquad \lambda = 1.52 \qquad \lambda = 1.69 \qquad \lambda = 1.86$$
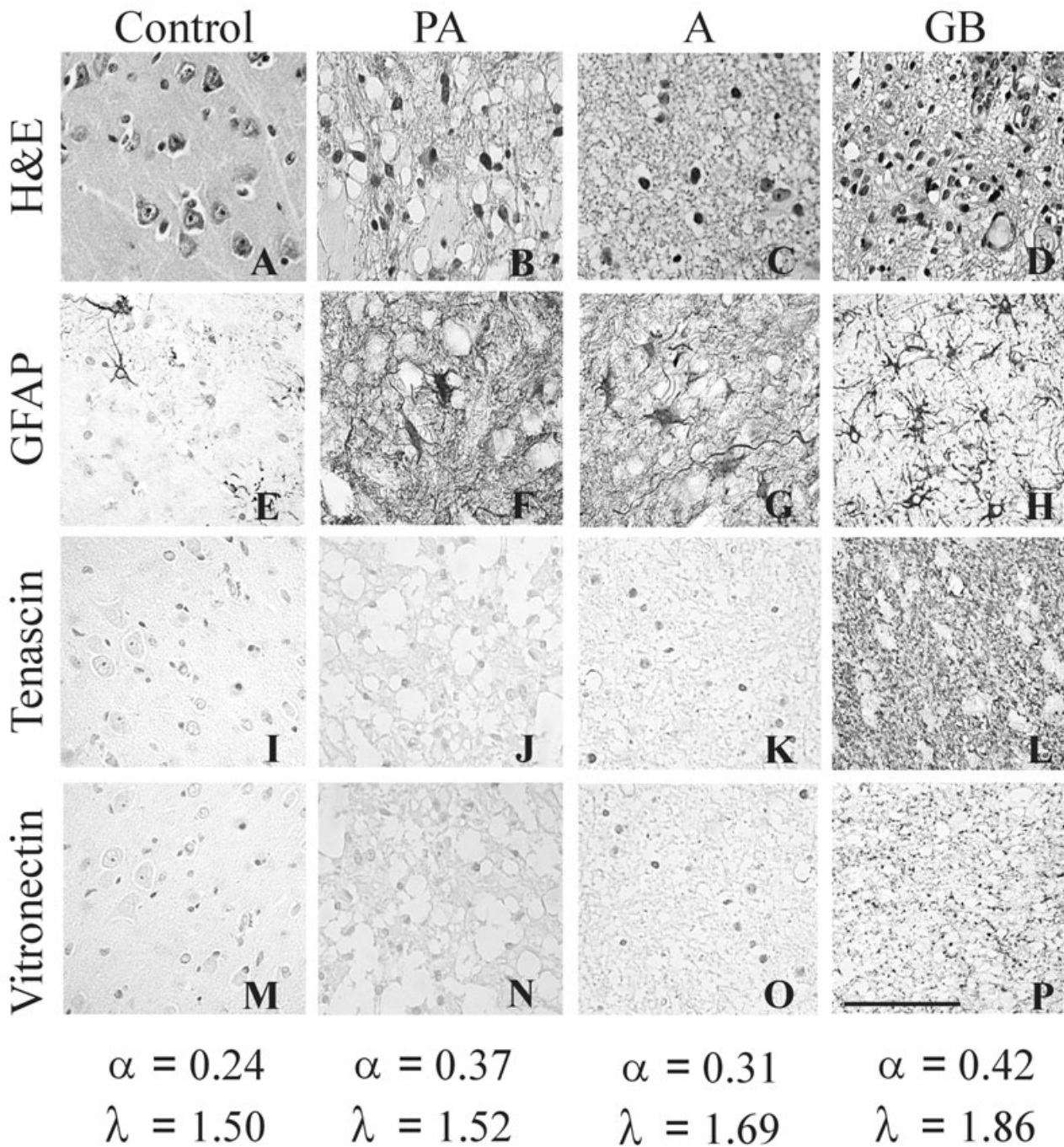
Figure 3. A comparison of tissue structure [**A–D**, haematoxylin-eosin (H&E) stain], the density of GFAP-positive tumour cell processes (**E–H**, immunoperoxidase stain; **E**, counterstained slightly with haematoxylin), the accumulation of tenascin (**I–L**, immunoperoxidase stain, **I–K**, counterstained slightly with haematoxylin) and vitronectin (**M–P**, immunoperoxidase stain, **M–O**, counterstained slightly with haematoxylin) in the extracellular space (ECS), and the ECS diffusion parameters (α, ECS volume fraction; λ, tortuosity). Scale bar (**A–P**) = 40 µm. PA, pilocytic astrocytoma (case 5); A, astrocytoma (case 12); GB, glioblastoma (case 20).
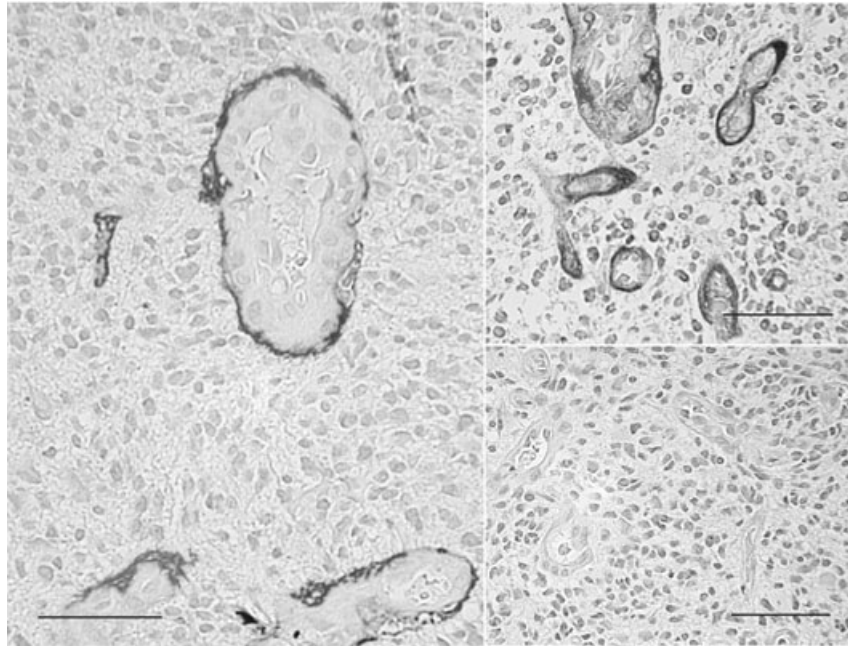
Figure 4. Immunoperoxidase staining for laminin localized in the subendothelial basement membranes of hyperplastic blood vessels of a glioblastoma (case 17, counterstained slightly with haematoxylin). Inset (upper): the same case, immunoperoxidase staining for type IV collagen (counterstained slightly with haematoxylin). Inset (lower): negative immunoperoxidase staining for fibronectin (counterstained slightly with haematoxylin). Scale bars = 50 μm.

in the subendothelial basement membranes of all blood vessels; collagen types II, V and VI were observed in the adventitia of clusters of hyperplastic tumour blood vessels in all glioblastoma cases (not shown). Collagen types I and III were not observed in high-grade astrocytomas.

In comparison with low-grade astrocytic tumours, both α and λ were significantly more increased in high-grade astrocytomas (MW; $P < 0.001$ and $P < 0.05$, respectively) than in low-grade astrocytomas (see Table 2).

Correlative analysis

The expression of the studied ECM glycoproteins in tissue samples obtained from patients with astrocytic tumours of different grades is summarized in Table 2, together with proliferation markers, tumour cell density, the density of GFAP-positive tumour cell processes and the ECS diffusion parameter values of the respective tumours.

The correlation between all possible combinations of pairs of variables reflecting cell density, the proliferative activity of diffuse infiltrating astrocytomas (WHO grade II–IV) and the diffusion parameters was examined statistically and is summarized in Table 3. Data from case 13

Table 3. Statistical correlation between extracellular space (ECS) diffusion parameters (ECS volume fraction α; tortuosity λ), tumour cell density (TCD) and markers of tumour proliferative activity: MIB-1 labelling index (MIB-1), topoisomerase II-α labelling index (topo-IIα) and mitotic activity (MA, mitotic count per 10 high-power fields). Spearman's rank correlation analysis (with correlation coefficient estimate, *r*)

		TCD	MA	MIB-1	topo-IIα	α
MA	*r*	0.68	–	–	–	–
	P	<0.001				
MIB-1	*r*	0.66	0.94	–	–	–
	P	<0.001	<0.0005			
topo-IIα	*r*	0.65	0.97	0.98	–	–
	P	<0.001	<0.0005	<0.0005		
α	*r*	0.69	0.91	0.88	0.93	–
	P	<0.001	<0.0005	<0.0005	<0.0005	
λ	*r*	0.26	0.36	0.41	0.40	0.14
	P	NS	NS	<0.05	<0.05	NS

NS, not significant.

were not incorporated into the analysis. The analysis revealed a strong positive correlation between increasing ECS volume fraction and increasing cellularity and proliferative activity. A similar relationship was found between increasing tortuosity and increasing proliferative LIs;

however, the tortuosity changes were independent of tumour cell density.

The relationship between the expression of the ECM glycoprotein tenascin and both tortuosity and ECS volume fraction in diffusely infiltrating astrocytomas (WHO grade II–IV) is shown in Figure 5. Both the ECS volume fraction and the tortuosity were significantly increased in tumours producing tenascin (cases 15–17, 19–22, 24, 25) (mean $\alpha = 0.47 \pm 0.02$, $\lambda = 1.75 \pm 0.03$) when compared with tenascin-negative tumours (mean $\alpha = 0.37 \pm 0.01$, $\lambda = 1.50 \pm 0.04$) (MW; $P < 0.05$ and $P < 0.003$, respectively). No statistically significant relationships between changes in volume and tortuosity and the other ECM glycoproteins that were overexpressed in high-grade gliomas (vitronectin and collagen types II, V and VI) were found.

Discussion

The ECS diffusion parameters investigated in our study enable one to quantify the exact volume of the ECS and to describe the complex of diffusion hindrances caused by cell processes and by the ECM in the ECS of the tissues, that is, the tortuosity. It has been repeatedly shown that the ECS diffusion parameters in central nervous system tissue slices obtained from experimental animals do not significantly differ from those determined in animals *in vivo* [14,15]. We can therefore assume that data from human tissue slices reflect the situation in the human brain *in vivo*.

Although the characteristic hypercellularity of brain neoplasms would seem to predict a reduced intercellular

space in tumour tissue, a varying degree of ECS enlargement in brain tumours was shown earlier [19,20] and confirmed in our previous study [8] across a spectrum of different brain tumours, including astrocytomas, ependymomas, oligodendrogliomas and medulloblastomas, and has been confirmed again in the current study. In addition to factors such as the ability of tumour cells to adhere to and migrate along the existing ECM [21], the migratory capacity of tumour cells may also be dependent on the ability of the tumour to create space for migrating cells. There are several factors that may contribute to an enlargement of the ECS: the degradation of the ECM by metalloproteinases produced by tumour cells [22], a loss of gap junctions associated with the inability of cells to regulate either their own or the extracellular volume [23], or the excitotoxic effect of glutamate, which reaches high concentrations in gliomas as a result of failed glutamate uptake [24]. The positive correlation between extensive intercellular tenascin deposits and an enlarged ECS volume suggests that another mechanism leading to ECS volume fraction increase is the enlargement of the intercellular space by overexpressed ECM components. The studied pilocytic astrocytomas had, when compared with grade II astrocytomas, a larger ECS volume fraction in spite of their lower grade and slower growth. This might be owing to the enlargement of the ECS by microcysts, which were consistently observed during light microscopic examination of these tumours. Based on our observations, the microcysts might be filled by a mucinous fluid of low density without any larger structural glycoproteins, which reflects the low tortuosity of the ECS in these tumours.

The observed ECS volume increase in high-grade gliomas was not associated with a decrease in tortuosity but rather with a significant tortuosity increase. Several factors that could possibly contribute to these changes have been investigated in our study, that is, cell density, fibrillary nets of GFAP-positive tumour cell processes, the hyperplastic vasculature of the tumours and the qualitative and quantitative changes in the composition of the ECM. Surprisingly, although we found a correlation between increased cell density and an enlarged ECS volume fraction, there was no obvious relationship between cell density and tortuosity. Furthermore, tortuosity seems to be only slightly influenced by the presence of hyperplastic vasculature in a tumour. Our data indicate that the hindrances to diffusion in the ECS of low-grade tumours are created by the network of GFAP-positive fibrillary pro-
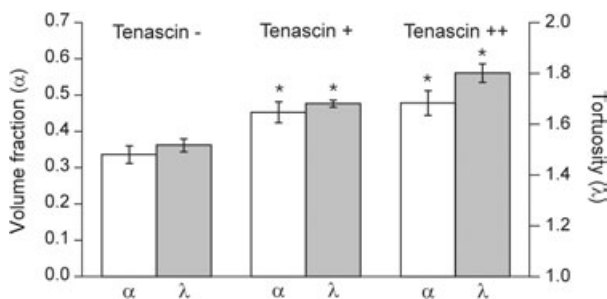
Figure 5. Graphs showing the increase in extracellular space (ECS) volume fraction (α) and tortuosity (λ) in astrocytic tumours with a small (tenascin +) or large (tenascin ++) accumulation of tenascin in the ECS compared to the diffusion parameters of tenascin-negative tumours (tenascin –). Stars indicate significant differences in the diffusion parameters α and λ between tenascin-positive and tenascin-negative tumours.

cesses of the tumour cells. A similar increase in ECS tortuosity was demonstrated previously in rats to be the result of postwounding astrogliosis [7]. On the other hand, we showed that shorter fibrillary processes of the tumour cells are of less importance in high-grade astrocytic tumours, where the major contributor to the tortuosity increase is probably the overexpression of ECM glycoproteins.

Changes in ECM composition have been intensively studied in tissue cultures of glioma cell lines [12]. However, because of extensive clonal selection and transdifferentiation in the cultures, mesenchymal features arise with an extensive ECM production [25–27], and the results obtained by such experiments do not necessarily reflect the situation *in vivo*. Although the capacity of cultured glioma cells to produce laminin, fibronectin and collagen types I and III–V has been shown [26,28–31], no intercellular deposits of these molecules were found in our study. In the case of collagen types I and III, their presence was not observed anywhere in the tumour tissue; collagen types IV–VI were associated strictly with vascular elements of both normal and tumour tissue independently of the malignancy grade, which is in accordance with previous observations [28,32]. The expression of type II collagen in normal and neoplastic brain tissue appears to be a novel finding. This type of collagen is a structural component of cartilage [33]. We observed a weak collagen type II immunopositivity in the adventitia of both normal larger blood vessels and the connective tissue of the meninges. Fibronectin and laminin were reported to be structural glycoproteins present in the vascular basement membrane of normal and tumour blood vessels [29,34]. The presence of these two glycoprotein was observed in that location in our study. However, similarly to Higuchi *et al*. [34], we found a significant decrease in fibronectin accumulation with increasing tumour grade. In contrast to Oz *et al*. [35], we did not observe such a correlation in the case of laminin, which was present in all the normal and tumour blood vessels examined.

From the investigated spectrum of ECM components, only tenascin together with vitronectin were found to be present in the ECS surrounding the tumour cells. In agreement with Gladson and Cheresh [36], we found vitronectin deposits in the ECS of some of the most malignant astrocytic tumours. However, the amount of vitronectin produced was limited, and therefore its possible effect on tortuosity could not be demonstrated. In contrast, there was a large amount of tenascin, a large glycoprotein typically forming a hexabrachion structure [37], detected in both the ECS and the perivascular tissues of the high-grade gliomas in our series, a finding in agreement with earlier data from both tissue culture and *in situ* studies [34,38,39]. Although tenascin is usually reported as being absent in the developed brain [37,40], our study in normal brain tissue revealed clearly distinguishable deposits of this glycoprotein in the glial limitans externa, and a weak positivity was also detected in the ECS of the white matter. A correlation between tenascin production and the malignancy or angiogenesis of tumours was recently clearly demonstrated [35,38,41,42] and can now be confirmed by our data as well. Moreover, based on our results, we suggest that the accumulation of this glycoprotein in the intercellular spaces is one of the major factors leading to the critical increase in ECS tortuosity and, at the same time, may contribute to the enlargement of the ECS. Additional evidence for this hypothesis comes from our recent findings that revealed decreased ECS volume and tortuosity in tenascin-knockout mice [43].

Other components of the brain ECM, such as glycosaminoglycans and proteoglycans (above all hyaluronate and chondroitin sulphate), have been demonstrated to be present in increased amounts in glial tumours [44,45]. Although these ECM components were not investigated in our study, we can speculate that this may not necessarily reflect the ability of tumour cells to produce these substances in excess, but rather may only mirror indirectly an enlarged ECS filled with the mucoid ground substances of the brain ECM that are known to be ubiquitous in the central nervous system [11,46].

In conclusion, our study demonstrates that with increasing malignancy of astrocytic tumours, there is a critical increase in the volume of the ECS accompanied by increased tortuosity owing to the production of ECM glycoproteins, mostly of tenascin. At present, new therapeutic approaches for the localized delivery of therapeutic agents to brain tumours [47,48] are being brought to clinical usage. The changes in the volume, geometry and composition of the tumour tissue ECS reported in this study, especially in tenascin-positive tumours, are of major importance, as they can critically impair the diffusion of therapeutic agents into tumour tissue and may thus contribute to their reduced effectiveness in some cases.

Acknowledgements

References

1 Giese A, Rief MD, Loo MA, Berens ME. Determinants of human astrocytoma migration. *Cancer Res* 1994; **54**: 3897–904

2 Goldbrunner RH, Bernstein JJ, Tonn JC. Cell-extracellular matrix interaction in glioma invasion. *Acta Neurochir (Wien)* 1999; **141**: 295–305

3 Sykova E, Mazel T, Vargova L, Vorisek I, Prokopova-Kubinova S. Extracellular space diffusion and pathological states. *Prog Brain Res* 2000; **125**: 155–78

4 Sykova E. Glial diffusion barriers during aging and pathological states. *Prog Brain Res* 2001; **132**: 339–63

5 Nicholson C, Sykova E. Extracellular space structure revealed by diffusion analysis. *Trends Neurosci* 1998; **21**: 207–15

6 Nicholson C, Phillips JM. Ion diffusion modified by tortuosity and volume fraction in the extracellular microenvironment of the rat cerebellum. *J Physiol* 1981; **321**: 225–57

7 Roitbak T, Sykova E. Diffusion barriers evoked in the rat cortex by reactive astrogliosis. *Glia* 1999; **28**: 40–8

8 Vargova L, Homola A, Zamecnik J, Tichy M, Benes V, Sykova E. Diffusion parameters of the extracellular space in human gliomas. *Glia* 2003; **42**: 77–88

9 Sykova E, Mazel T, Simonova Z. Diffusion constraints and neuron-glia interaction during aging. *Exp Gerontol* 1998; **33**: 837–51

10 Sykova E, Vargova L, Prokopova S, Simonova Z. Glial swelling and astrogliosis produce diffusion barriers in the rat spinal cord. *Glia* 1999; **25**: 56–70

11 Chintala SK, Rao JK. Invasion of human glioma: role of extracellular matrix proteins. *Front Biosci* 1996; **1**: d324–39

12 Gladson CL. The extracellular matrix of gliomas: modulation of cell function. *J Neuropathol Exp Neurol* 1999; **58**: 1029–40

13 Kleihues P, Cavenee WK, eds. *WHO Classification of Tumours: Pathology and Genetics of Tumours of the Nervous System*. Lyon: IARC Press, 2000; 10–51

14 Prokopova S, Vargova L, Sykova E. Heterogeneous and anisotropic diffusion in the developing rat spinal cord. *Neuroreport* 1997; **8**: 3527–32

15 Lehmenkuhler A, Sykova E, Svoboda J, Zilles K, Nicholson C. Extracellular space parameters in the rat neocortex and subcortical white matter during postnatal development determined by diffusion analysis. *Neuroscience* 1993; **55**: 339–51

16 Sykova E. Ion-selective electrodes. In *Monitoring Neuronal Cells: a Practical Approach*. Ed. J Stamford. New York: Oxford University Press, 1992; 261–82

17 Gerdes J, Becker MH, Key G, Cattoretti G. Immunohistological detection of tumour growth fraction (Ki-67 antigen) in formalin-fixed and routinely processed tissues. *J Pathol* 1992; **168**: 85–6

18 Holden JA, Townsend JJ. DNA topoisomerase II-alpha as a proliferation marker in astrocytic neoplasms of the central nervous system: correlation with MIB1 expression and patient survival. *Mod Pathol* 1999; **12**: 1094–100

19 Bakay L. The extracellular space in brain tumours. II. The sucrose space. *Brain* 1970; **93**: 699–708

20 Matthews CM, Molinaro G. A study of the relative value of radioactive substances used for brain tumor localization and of the mechanism of tumor: brain concentration. Uptake in transplantable fibrosarcoma, brain and other organs in the rat. *Br J Exp Pathol* 1963; **44**: 260–77

21 Bolteus AJ, Berens ME, Pilkington GJ. Migration and invasion in brain neoplasms. *Curr Neurol Neurosci Rep* 2001; **1**: 225–32

22 Chintala SK, Tonn JC, Rao JS. Matrix metalloproteinases and their biological function in human gliomas. *Int J Dev Neurosci* 1999; **17**: 495–502

23 Quist AP, Rhee SK, Lin H, Lal R. Physiological role of gap-junctional hemichannels. Extracellular calcium-dependent isosmotic volume regulation. *J Cell Biol* 2000; **148**: 1063–74

24 Ye ZC, Sontheimer H. Glioma cells release excitotoxic concentrations of glutamate. *Cancer Res* 1999; **59**: 4383–91

25 Mahesparan R, Tysnes BB, Read TA, Enger PO, Bjerkvig R, Lund-Johansen M. Extracellular matrix-induced cell migration from glioblastoma biopsy specimens in vitro. *Acta Neuropathol (Berl)* 1999; **97**: 231–9

26 McKeever PE, Fligiel SE, Varani J, Castle RL, Hood TW. Products of cells cultured from gliomas. VII. Extracellular matrix proteins of gliomas which contain glial fibrillary acidic protein. *Lab Invest* 1989; **60**: 286–95

27 Paulus W, Huettner C, Tonn JC. Collagens, integrins and the mesenchymal drift in glioblastomas: a comparison of biopsy specimens, spheroid and early monolayer cultures. *Int J Cancer* 1994; **58**: 841–6

28 Bellon G, Caulet T, Cam Y, Pluot M, Poulin G, Pytlinska M, Bernard MH. Immunohistochemical localisation of macromolecules of the basement membrane and extracellular matrix of human gliomas and meningiomas. *Acta Neuropathol (Berl)* 1985; **66**: 245–52

29 Chintala SK, Sawaya R, Gokaslan ZL, Fuller G, Rao JS. Immunohistochemical localization of extracellular matrix proteins in human glioma, both in vivo and in vitro. *Cancer Lett* 1996; **101**: 107–14

30 Rucklidge GJ, Dean V, Robins SP, Mella O, Bjerkvig R. Immunolocalization of extracellular matrix proteins during brain tumor invasion in BD IX rats. *Cancer Res* 1989; **49**: 5419–23

31 Tysnes BB, Mahesparan R, Thorsen F, Haugland HK, Porwol T, Enger PO, Lund-Johansen M, Bjerkvig R. Laminin expression by glial fibrillary acidic protein positive cells in human gliomas. *Int J Dev Neurosci* 1999; **17**: 531–9

32 Paulus W, Roggendorf W, Schuppan D. Immunohistochemical investigation of collagen subtypes in human glioblastomas. *Virchows Arch* 1988; **413**: 325–32

33 Eyre D. Collagen of articular cartilage. *Arthritis Res* 2002; **4**: 30–5

34 Higuchi M, Ohnishi T, Arita N, Hiraga S, Hayakawa T. Expression of tenascin in human gliomas: its relation to histological malignancy, tumor dedifferentiation and angiogenesis. *Acta Neuropathol (Berl)* 1993; **85**: 481–7

35 Oz B, Karayel FA, Gazio NL, Ozlen F, Balci K. The distribution of extracellular matrix proteins and CD44S expression in human astrocytomas. *Pathol Oncol Res* 2000; **6**: 118–24

36 Gladson CL, Cheresh DA. Glioblastoma expression of vitronectin and the alpha v beta 3 integrin. Adhesion mechanism for transformed glial cells. *J Clin Invest* 1991; **88**: 1924–32

37 Crossin KL. Tenascin: a multifunctional extracellular matrix protein with a restricted distribution in development and disease. *J Cell Biochem* 1996; **61**: 592–8

38 Kim CH, Bak KH, Kim YS, Kim JM, Ko Y, Oh SJ, Kim KM, Hong EK. Expression of tenascin-C in astrocytic tumors: its relevance to proliferation and angiogenesis. *Surg Neurol* 2000; **54**: 235–40

39 Zagzag D, Friedlander DR, Miller DC, Dosik J, Cangiarella J, Kostianovsky M, Cohen H, Grumet M, Greco MA. Tenascin expression in astrocytomas correlates with angiogenesis. *Cancer Res* 1995; **55**: 907–14

40 Joester A, Faissner A. The structure and function of tenascin in the nervous system. *Matrix Biol* 2001; **20**: 13–22

41 Herold-Mende C, Mueller MM, Bonsanto MM, Schmitt HP, Kunze S, Steiner HH. Clinical impact and functional aspects of tenascin-C expression during glioma progression. *Int J Cancer* 2002; **98**: 362–9

42 Rascher G, Fischmann A, Kroger S, Duffner F, Grote EH, Wolburg H. Extracellular matrix and the blood-brain barrier in glioblastoma multiforme: spatial segregation of tenascin and agrin. *Acta Neuropathol (Berl)* 2002; **104**: 85–91

43 Vorisek I, Antonova T, Mazel T, Hajek M, Sykova E. Diffusion and extracellular space volume fraction in the brain of mice lacking tenascin-R or HNK1 sulfotransferase. *Proc Intl Soc Mag Reson Med* 2003; **11**: 1983

44 Delpech B, Maingonnat C, Girard N, Chauzy C, Maunoury R, Olivier A, Tayot J, Creissard P. Hyaluronan and hyaluronectin in the extracellular matrix of human brain tumour stroma. *Eur J Cancer* 1993; **29A**: 1012–17

45 Knudson W, Biswas C, Li XQ, Nemec RE, Toole BP. The role and regulation of tumour-associated hyaluronan. *Ciba Found Symp* 1989; **143**: 150–9

46 Margolis RK, Margolis RU. Nervous tissue proteoglycans. *Experientia* 1993; **49**: 429–46

47 Read TA, Thorsen F, Bjerkvig R. Localised delivery of therapeutic agents to CNS malignancies: old and new approaches. *Curr Pharm Biotechnol* 2002; **3**: 257–73

48 Reardon DA, Akabani G, Coleman RE, Friedman AH, Friedman HS, Herndon JE, Cokgor I, McLendon RE, Pegram CN, Provenzale JM, Quinn JA, Rich JN, Regalado LV, Sampson JH, Shafman TD, Wikstrand CJ, Wong TZ, Zhao XG, Zalutsky MR, Bigner DD. Phase II trial of murine (131)I-labeled antitenascin monoclonal antibody 81C6 administered into surgically created resection cavities of patients with newly diagnosed malignant gliomas. *J Clin Oncol* 2002; **20**: 1389–97